




High mechanical stable flexible transparent conductive In-doped CdO thin film deposited at low temperature on PET substrate

Zishu Zhu¹, Wei Zhu^{1,*}, Yanpu Chen¹, Pingping Ma¹, Haolei Zhou¹, LirenLou¹, and Guanzhong Wang^{1,*} 

¹Key Laboratory of Strongly-Coupled Matter Physics, Chinese Academy of Sciences, and Department of Physics, University of Science and Technology of China, Hefei 230026, Anhui, People's Republic of China

Received: 4 June 2021

Accepted: 7 January 2022

Published online:
22 January 2022

© The Author(s), under exclusive licence to Springer Science+Business Media, LLC, part of Springer Nature 2022

ABSTRACT

To explore new kind of flexible transparent conductive oxide films for application in flexible optoelectronic devices, In-doped CdO thin films were synthesized by radio frequency magnetron sputtering on thin polyethylene terephthalate substrates at low temperature. The effects of growth time and temperature on the resistance and transmittance of In-doped CdO films were studied in detail for the first time. It is demonstrated that the sheet resistance of the film deposited at 100 °C for 20 min was 96.9 Ω/cm² for the as-grown sample and increased about 6.4% after experienced 500 bending cycles. The results demonstrate that the In-doped CdO films possess not only excellent optoelectronic properties but also high mechanical stability. In-doped CdO films show great potential to be applied in wearable electronics, transparent devices, solar cells and so forth.

1 Introduction

Flexible optoelectronic devices have received more commercial and academic attention. In these devices components [1], for example, Indium Tin Oxide (ITO), an excellent material with good optoelectronic properties and chemical stability, has been widely used in various devices, such as in liquid crystal display (LCD) [2–7]. However, ITO films with excellent electrical properties need to be prepared above 150 °C, but at this temperature, the commonly used

organic substrates will be deformed, which limits the substrate choice. On the other hand, the rising price of ITO is another disadvantage [2, 8]. ITO films, owing to their brittleness, also show low mechanical stability [9]. It is desirable to find a new material to substitute ITO in flexible devices [10–13].

As a potentially alternative material to ITO, doped CdO has attracted increasing attention recently. It is an n-type semiconductor with high mobility (> 100 cm²/V s) and high transmittance (75–98% in visible light region) [5, 14, 15]. The high transmittance spectral region of it can be adjusted easily by doping

Address correspondence to E-mail: zhuw@ustc.edu.cn; gzwang@ustc.edu.cn

various elements with different concentrations [14–21]. In view of these facts, it is thought that the doped CdO is suitable to be applied as transparent conductive materials in various optoelectronic devices [5]. The price of CdO is also much cheaper than the ITO's [8]. It is more important that highly conductive and transparent doped CdO film can be formed easily at room temperature (RT) by using RF magnetron sputtering system on various flexible organic substrates [5, 22–24], which suggests that CdO is promising for application in flexible optoelectronic devices.

It is reported that the resistivity of CdO films doped with B, Si, Ge, W are $1.56 \times 10^{-4} \Omega \text{ cm}$ [25], $1.94 \times 10^{-4} \Omega \text{ cm}$ [26], $2.76 \times 10^{-4} \Omega \text{ cm}$ [27], $3.85 \times 10^{-4} \Omega \text{ cm}$ [28], respectively. While the resistivity of CdO film doped with 5% In is $1.3 \times 10^{-4} \Omega \text{ cm}$ [5], which is lower than that of the doped films shown above. However, there are few specific studies on the properties of the CdO-based flexible transparent films reported. In order to clarify the effects of growth conditions on the optical and electrical properties of the film, In-doped CdO films were deposited on ordinary polyethylene terephthalate (PET) films by radio frequency (RF) magnetron sputtering under various conditions. Then the optoelectronic properties and mechanical stability of the films prepared under different conditions were characterized. It is reported that the films with the In concentration around 5% prepared under proper conditions exhibited good optoelectronic properties [5, 29]. In this work, the effect of synthesis temperature and time on the conductivity, transparency and mechanical stability of In-doped CdO films were studied in detail for the first time. 5% In-doped CdO films with good optical and electrical properties and high mechanical stability were synthesized, which satisfy well the requirements of application in flexible optoelectronic devices.

2 Experimental

In-doped CdO layers were deposited on thin PET films (0.0125 mm, purchased from Colleague Hardware) by RF sputtering using the JCP-350M2 high vacuum multi-target RF magnetron sputtering system. The sputtering targets CdO (99.99%) and In_2O_3 (99.99%) were purchased from Chinese New Metal Company. The PET substrates were cut into 2 cm^2

and ultrasonically cleaned with de-ionized water and methanol, respectively, each for 30 min. Then the substrates were rinsed by de-ionized water and dried with nitrogen.

Before the deposition, the chamber was pumped down to the base pressure $1.5 \times 10^{-3} \text{ Pa}$. The high purity Ar (99.99%) was then introduced into the chamber, controlled by a flow controller to fix the chamber's pressure at 0.5 Pa during the whole sputtering process. To synthesized 5% In-doped CdO films with good optoelectronic properties, the sputtering power of the CdO and the In_2O_3 targets were set at 100 W and 20 W respectively, which is base on the works published previously [5]. In order to study the influence of sputtering parameters on the optical and electrical properties of the films, different sputtering conditions were used to prepare the CdO films: the deposition time was varied from 10 to 30 min and the temperature of substrate was varied from 25 to 150 °C. Because PET films would wrinkle heavily at a temperature higher than 150 °C, the samples were not prepared at higher deposition temperature. The deposition parameters for different samples are presented in Table 1.

The properties of the deposited samples were characterized systematically. The crystalline structures of the deposited samples were measured by X-ray diffraction (XRD) (Rigaku Smartlab) using Cu K_α radiation source (wavelength 1.5418 Å). Thicknesses of the samples were measured by a J.A.Woollam Co., Inc. Ellipsometry Solutions M-2000U. Electrical properties were characterized at RT through Hall Effect in the van der Pauw configuration using an Ecopia HMS-5000 system with a 0.556 T permanent magnet. The elemental concentration analysis was carried out by Hitachi Co., Inc. Energy Dispersive Spectrometer (EDS) SU8220 and

Table 1 RF sputtering parameters for depositing In-doped CdO films

| Sample | Deposition temperature (°C) | | | | | |
|-----------------|-----------------------------|-----|-----|-----|-----|-----|
| | 25 | 50 | 75 | 100 | 125 | 150 |
| Deposition time | | | | | | |
| 10 min | A-1 | A-2 | A-3 | A-4 | A-5 | A-6 |
| 20 min | B-1 | B-2 | B-3 | B-4 | B-5 | B-6 |
| 30 min | C-1 | C-2 | C-3 | C-4 | C-5 | C-6 |

the oxidation state of films were analyzed by X-ray photoelectron spectroscopy (XPS) (ESCALAB 250).

3 Results and analysis

3.1 Film structure

Figure 1 shows the XRD patterns of the prepared films. The diffraction peaks near 33.0° and 38.3° can be attributed to the crystal planes of (111), (200) of cubic CdO (JCPDS card #75-0594), which indicates that the CdO films, deposited at temperature lower than 150°C , even at RT, crystallize well. However, ITO films with good crystallinity must be deposited above 300°C by sputtering, and most organic substrates will suffer damage under this temperature [30]. This result indicates that comparing to ITO films, In-doped CdO is more suitable for application in flexible optoelectronic devices.

For the samples with deposition time of 10 min, the XRD spectra Fig. 1a) exhibited two distinct peaks near 27.8° and 44.5° , which can be assigned to cubic In_2O_3 (310) and (422) (JCPDS card #76-0152), respectively. With longer deposition time, the peaks of In_2O_3 were weaker in the XRD patterns of the samples. It is suggested that In_2O_3 tend to form and crystallize near the surface of PET, while inside the deposited film In serves as dopant in the lattice of CdO, which cause the decreasing of the peak of In_2O_3 for samples with longer growth time.

It can also be seen from Fig. 1a–c that the relative intensities and the widths of the peaks varied with the deposition time. When the growth time was 20 min or 30 min, the CdO (200) peak was the most intensive one, showing the deposited CdO film predominantly with the c-axis perpendicular to the substrates. Nevertheless, for the samples of growth time 10 min, the preferential crystal orientation vertical to the substrates was CdO (111). The widths of

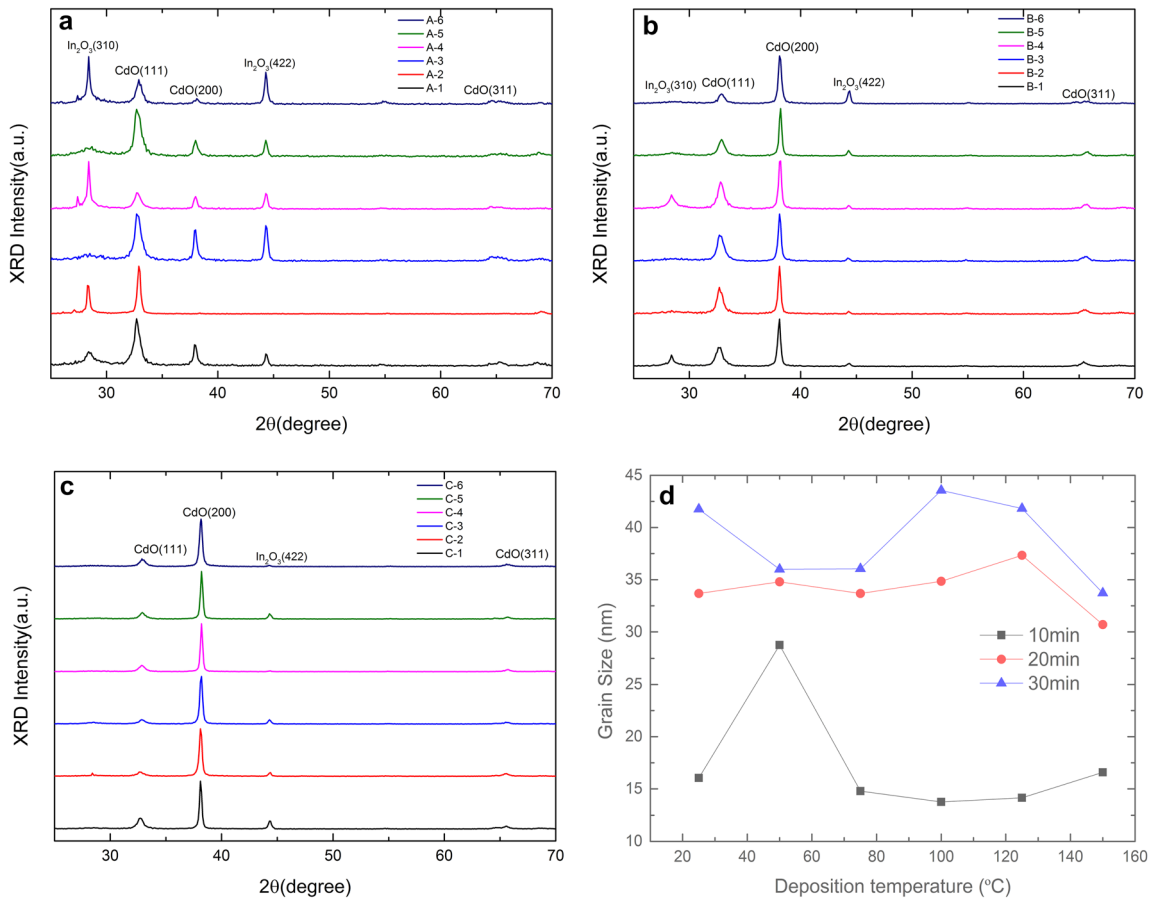


Fig. 1 a–c XRD patterns of the In-doped CdO films deposited on PET under various temperatures (see Table 1) for the same growth time of a 10 min, b 20 min and c 30 min. d shows the grain sizes of different samples, estimated by Scherrer formula

the peaks also were affected by the growth time, suggesting a variation of the grain size of the crystallite in the film with the film growth time. The average grain size in a polycrystal can be estimated by Scherrer formula:

$$D_{hkl} = \frac{K\lambda}{B_{hkl}\cos(\theta_{hkl})}, \quad (1)$$

where h , k and l are the indices of lattice planes, D_{hkl} is the grain size of a crystal in the direction perpendicular to hkl direction, B_{hkl} is the full width at half-maximum of the diffraction peak (hkl), λ is the wavelength of X-ray and θ_{hkl} is the Bragg angle. The Scherrer constant K is usually taken as 0.93 [31]. Figure 1d) shows the grain sizes estimated for three series samples of different growth times and temperatures. In the estimation the main peaks were used (111) for samples with deposition time of 10 min and (200) for the samples with longer growth time. It can be seen that the estimated grain size increases with the growth time. These results also suggest that, the crystallinity of the region near the PET substrate in the deposited In-doped CdO film was worse than that of the inside of the film, which may be caused by the amorphousness of PET, substrate, decreasing the crystallinity of the sample. Higher crystallinity means less grain boundaries in the samples, resulting in higher carrier mobility of the films.

In order to confirm that the existence of In_2O_3 crystals in the initial deposition region of the samples, XPS for different samples were taken and the results are shown in Fig. 2. For the oxygen spectra, the strongest peak around 532 eV can be attributed to O^{2-} in CdO crystal [32]. For sample A-4 and B-4 with less growth time, another peak around 529 eV can be detected, which can be attributed to O^{2-} in In_2O_3 crystal [33]. But for the spectra of sample C-4 with growth time of 30 min, this peak is much weaker. Figure 2 d) shows two peaks of In^{3+} $3d_{3/2}$ and $3d_{5/2}$ located around 452 eV and 445 eV respectively for the samples deposited under 100 °C with various growth time [33], which confirms the existence of In element. Fig.S1 in supporting materials shows the HRTEM image of sample C-4, in which In_2O_3 grains were observed near the PET substrates. The results confirm that at the beginning stage of deposition In_2O_3 tended to form separate nano-particles. As the film growing thicker, In atoms preferred to dope in the CdO crystal lattice. It is suggested that In_2O_3

grains are easier to form near the amorphous PET substrate in the initial stage of deposition, however, the In^{3+} ions tended to doped into CdO lattice when the CdO crystallized well in the subsequent film growing.

The samples can be referred as to $\text{Cd}_{1-x}\text{In}_x\text{O}$, and x means the cation ratios of In^{3+} . Figure 3 shows the EDS results for the samples with deposition time of 30 min but different deposition temperature. The x changed from 0.051 to 0.058, which is what we required. The small variation indicated that the change of structure and electrical properties of samples were not caused by the cation ratios of In^{3+} .

The thicknesses of the films were measured by an ellipsometer. The thickness and deposition rate of samples are shown in Fig. 4. With increasing temperature, the average deposition rate is slightly decreased for the samples with deposition time of 10 min or 20 min. But for the samples with a deposition time of 30 min, the deposition rate increased with deposition temperature. Combined with the XRD and the XPS results, this result can be ascribed to the different growing surface in the beginning and subsequent growth stage. In atoms preferentially form In_2O_3 grains on the amorphous PET substrate at the beginning, and tend to dope in the CdO lattice when the CdO dominates most growth surface.

3.2 Optical properties

Figure 5a represents the transmittance spectra, recorded in the spectral region 350 nm–1800 nm, of the In-doped CdO films on PET with different deposition conditions, where the contribution from PET substrates were excluded as background. The oscillatory feature shown in the spectra was caused by optical interference of films [34]. All the samples showed low transmittance in the ultraviolet (UV) region and the transmittance raised sharply around 400 nm. It is noteworthy that the B-4 showed the highest transmittance, being close to 100% at 700 nm. According to Fig. 5b, which shows the average transmittance of each sample, the average transmittances in the range of 500 nm–900 nm are 82, 91 and 85% for samples A-4, B-4 and C-4, respectively. Comparing with other works showing transmittance from 75 to 88% [34], B-4 showed higher transmittance in infrared band. The above results demonstrate that these CdO films are well suitable to be used in optoelectronic devices. With growth time of 20 min,

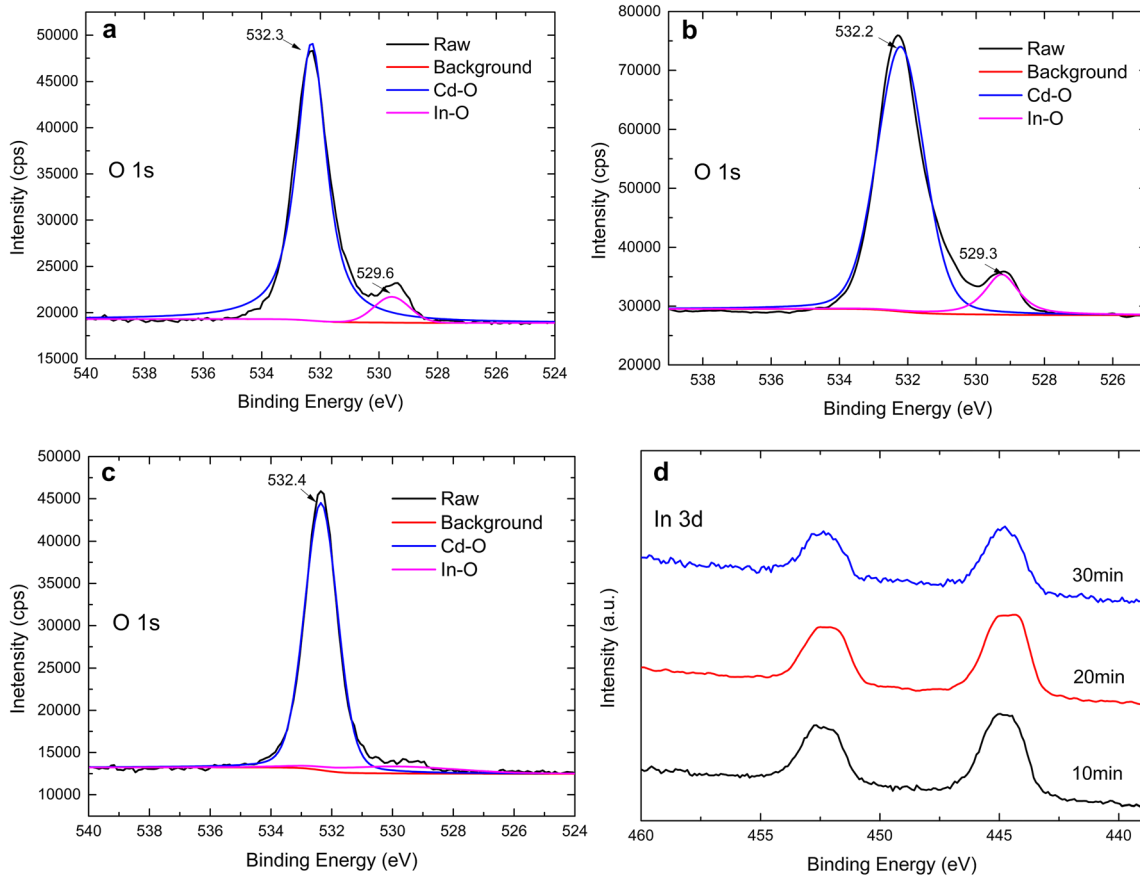


Fig. 2 XPS spectra of oxygen in O 1s region for sample **a** A-4, **b** B-4, **c** C-4, respectively. **d** The XPS spectra of indium in In 3d region for samples deposited under 100 °C with different deposition time

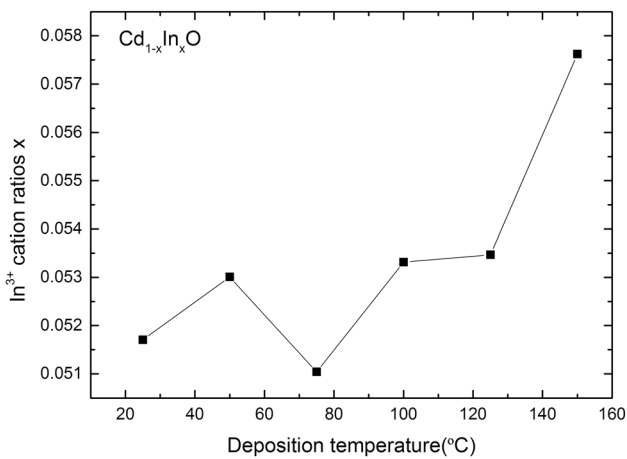


Fig. 3 Effects of the deposition temperature on the cation ratios of In^{3+} for the samples with deposition time of 30 min

samples not only had better crystallinity than samples with shorter growth time but also showed thinner thickness than samples with longer growth time. As the result, the sample with growth time of 20 min

shows highest average transmittance, as shown in Fig. 5b.

3.3 Electrical properties

Figure 6 shows the effect of deposition times and substrate temperatures on the electric properties of the films. According to Fig. 6a, the increasing of deposition temperature reduced the sheet resistance of the samples. For the samples with growth time of 20 min or 30 min, the mobility increase with deposition temperature when the temperature is less than 75 °C, as shown in Fig. 6b. These results can be explained by the change of the grain size in the samples, as shown in Fig. 1d. Higher deposition temperature leads to better crystalline quality of films with larger grain size, which means less grain boundary and hence reduces carrier scattering. But when the growth temperature is higher than 75 °C, the temperature and deposition time have little impact on mobility. This phenomenon could be

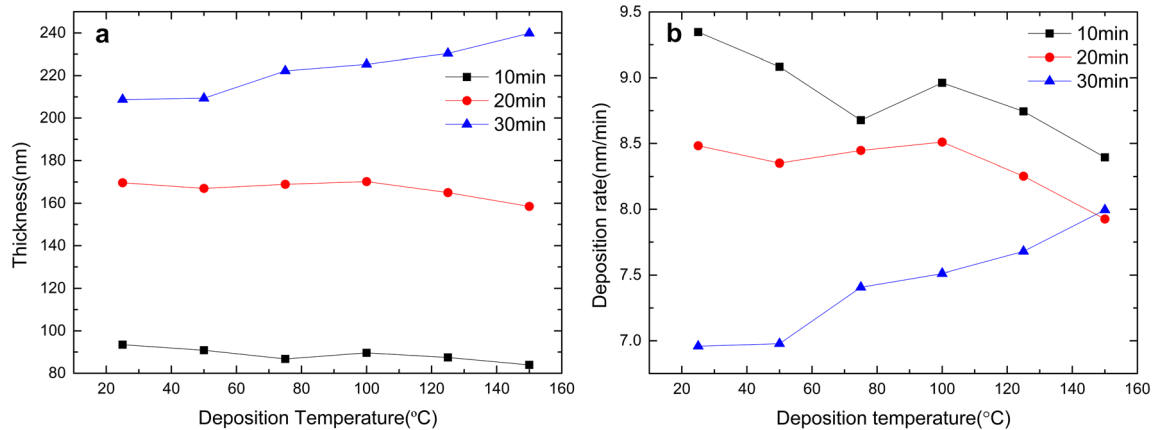


Fig. 4 Effects of the deposition temperature on **a** thickness, **b** deposition rate of samples with different deposition times

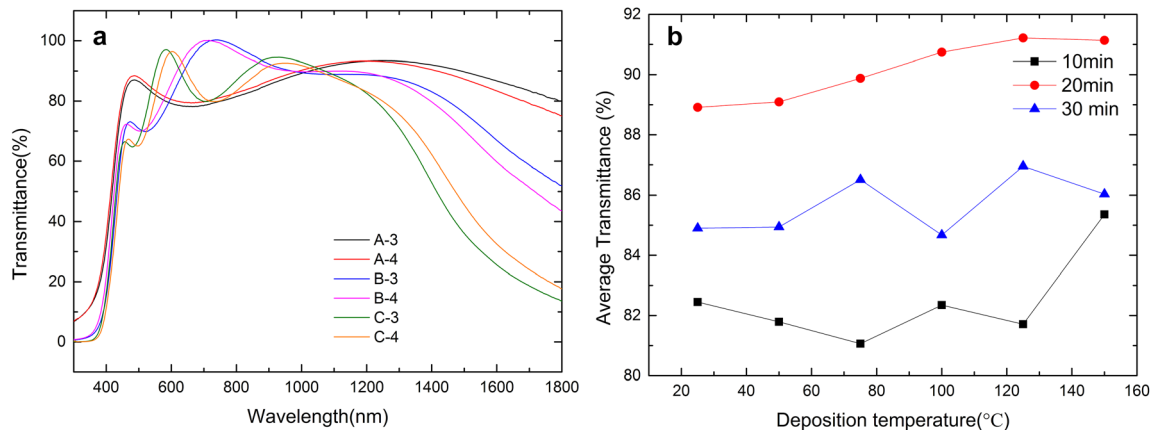


Fig. 5 **a** Transmittance spectra of samples deposited at different conditions. **b** Effects of deposition temperature on average transmittances in the range of 500 nm–900 nm

understood by considering the compensating effect of deposition temperature, the effect of expansion mismatch between PET and CdO. The thermal expansion coefficient of PET and CdO is $59.4 \mu\text{m}/\text{K}$ and $1.2 \mu\text{m}/\text{K}$, respectively. The great expansion mismatch would result in the high stress in In-doped CdO films as the deposited sample cooled down to RT and hence introduces more crystalline defects in the films, and consequently decreases the mobility. These two opposite temperature effects on mobility neutralize each other at the temperature beyond 75°C , leading to a weak dependence between mobility and deposition temperature. Figure 6c shows that higher deposition temperature increases carrier sheet concentration, which can be attributed to better crystallinity of the deposited films. It is not surprising that owing to their higher charge carrier concentration and mobility, films deposited with

higher deposition temperature show lower sheet resistance.

3.4 Mechanical stability

The electrical properties of the curved samples were measured using a Hall System as shown in Fig. 7, where the sample film was placed on a Teflon rod located on the sample platform and pressed by probes against the rod, causing the film bending at a curvature of the rod surface. Different curvatures can be achieved by using rods with different radiuses.

To study the mechanical stability, which means the stability in optoelectronic properties of the film upon bending, the relative sheet resistances R/R_0 of the films were measured under different bending curvatures, where R is the sheet resistance of the sample under bending and R_0 is the sheet resistance before

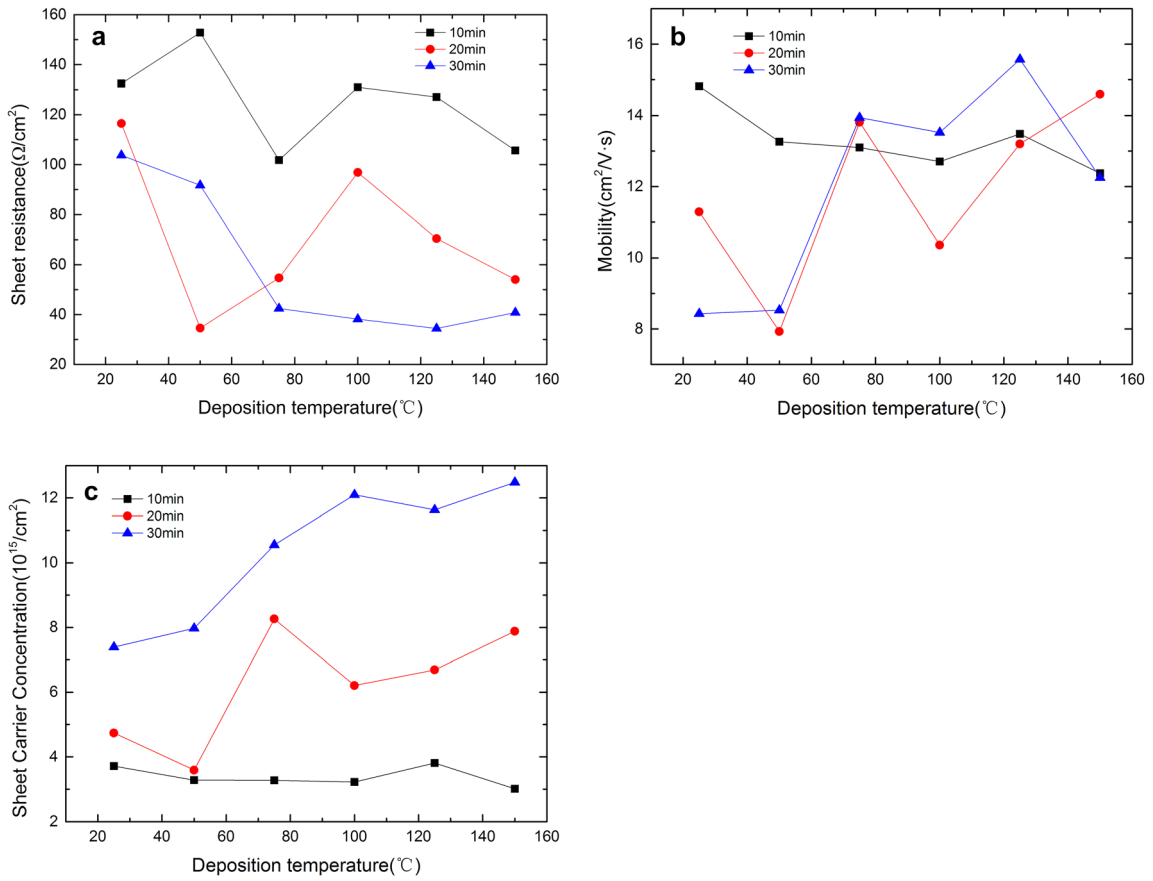


Fig. 6 Effects of the deposition temperature on **a** sheet resistance, **b** mobility, **c** sheet carrier concentration of samples with different deposition times

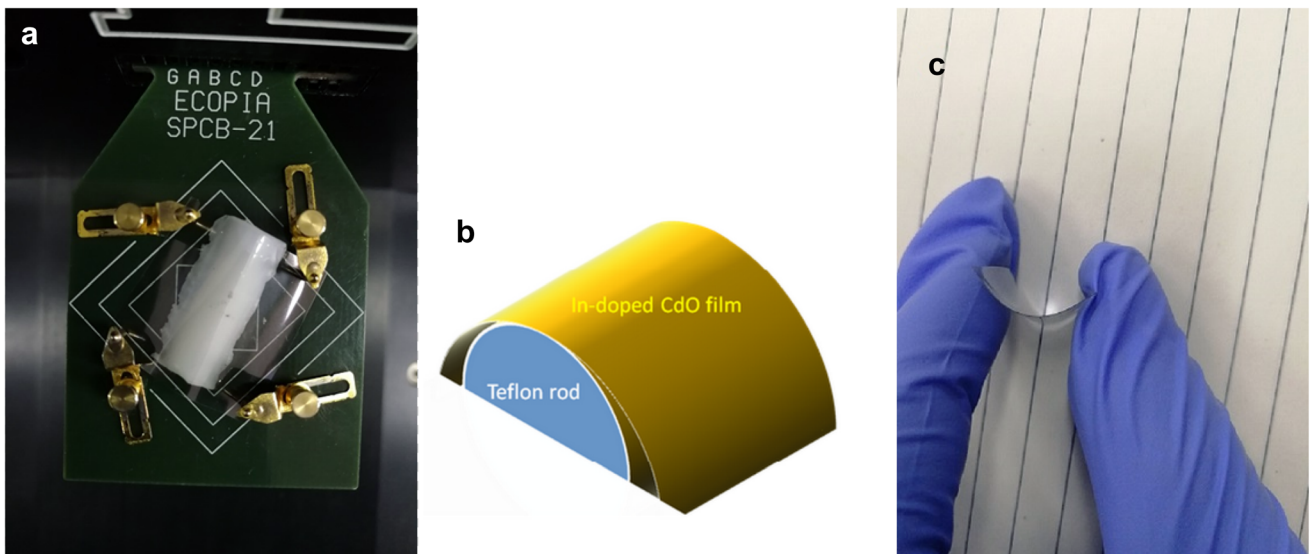


Fig. 7 a Diagram of the Hall system used to measure electrical properties of the curved films. During the test, four probes pressed the four corners of the sample and pushed the film against the Teflon rod, making the film out bent accordingly. **b** Schematic diagram of the film of given curvature for electric measurement.

c Showing the method used to bend the film. In the work the film was bent by fingers to a curvature of about 0.14 mm⁻¹ and then naturally unfolded, finishing a bending cycle. After multiple bending cycles the sample was used for electric properties testing

bending. Smaller variation in relative sheet resistance means better mechanical stability.

Figure 8 shows the relative sheet resistance of the films, deposited at various conditions, as functions of bending curvatures. All the samples showed constant resistance when the curvature was less than 0.06 mm^{-1} . However, for samples deposited at 25°C or 50°C , the resistance raised notably when the bending curvature exceeded 0.06 mm^{-1} , indicating the films had poor mechanical stability. But the mechanical stability of samples with deposition temperature from 75 to 125°C was much better. Even with high bending curvature 0.19 mm^{-1} , the relative resistance was still less than 200%. These phenomena can be interpreted by that high deposition temperature can promote the crystallinity of the film and enhance the adhesion between the film and PET, leading to better mechanical stability [3]. But the samples deposited at 150°C showed higher relative sheet resistance under the bending of the same

curvature, indicating that the film had worse crystallinity. This should be caused by the expansion mismatch between the PET substrate and the In-doped CdO film, inducing large inner stress in the In-doped CdO films during the cooling process. Similarly, under a considerable bending, large inner stress would be produced which would lead to more defects inside the film and degrade the electric properties of films.

The resistance change of the deposited samples after bending multiple cycles was tested, to see their mechanical stabilities. In the test each sample was bent convexly by fingers with a curvature of about 0.14 mm^{-1} , and then naturally unfolded, completing a bending cycle. After repeated this cycle for different times, the sheet resistances of the samples were measured. The obtained relationships between relative sheet resistance and the number of bending cycles for samples grown with different parameters are shown in Fig. 9.

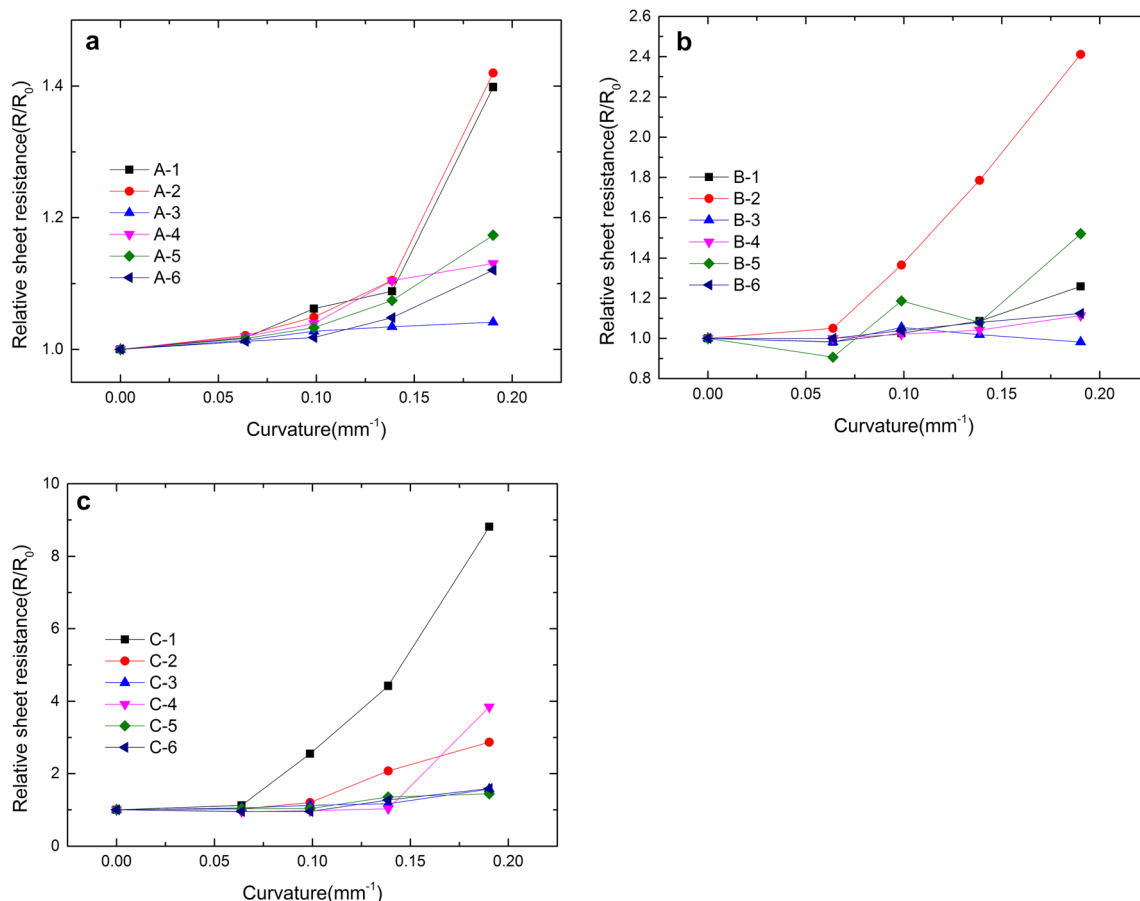


Fig. 8 Relative sheet resistance versus bending curvature for In-doped CdO film deposited on PET with different growth time of a 0.10 min, b 0.20 min, c 0.30 min

As shown in the Fig. 9, the relative sheet resistances of the films increase with the number of bending cycles. Among all the samples tested here the sample deposited at 100 °C with growth time 20 min (i.e. B4) showed lowest relative sheet resistance. It can be interpreted that increasing of deposition temperature can promote adhesion between films and substrates but also generate higher inner stress in the film. A sample deposited at 100 °C had good adhesion but the stress was still not very high, leading to its lowest relative sheet resistance. But for samples with growth time of 10 min, the increase in deposition temperature caused a rise in relative sheet resistance. It may be due the poor crystallinity of In-doped CdO films. Figure 9 also shows that with the same deposition temperature, samples with longer growth time of 30 min show higher relative sheet resistance. The reason is that higher internal stress would be introduced in the thicker film under the same bending curvature.

A suitable flexible conducting film should have both low sheet resistance and high mechanical stability. To clearly show the different behavior on the mechanical stability of the samples, as an example, the samples deposited at the temperature of 100 °C but with different growth times are compared in Fig. 10. It can be seen that B-4 shows a lower relative sheet resistance than that of A-4 and C-4 after 500 bending cycles. It indicates that the crystallinity of A-4 and C-4 is inferior to that of B-4, in other words more defects would exist in them, leading to degradation of film quality. This point is consistent to XRD results mentioned above. It is also noticed that the relative sheet resistance of sample C-4 increases more rapidly than A-4. As C-4 with higher thickness, the bending would generate higher inner stress and consequently make more defects formed in the film. As a result, the sheet resistance will rise more quickly with the bending cycles. The insert of Fig. 10 shows that after 500 bending cycles, R/R_0 of B-4 just increases to 1.064, just slightly larger than that of the

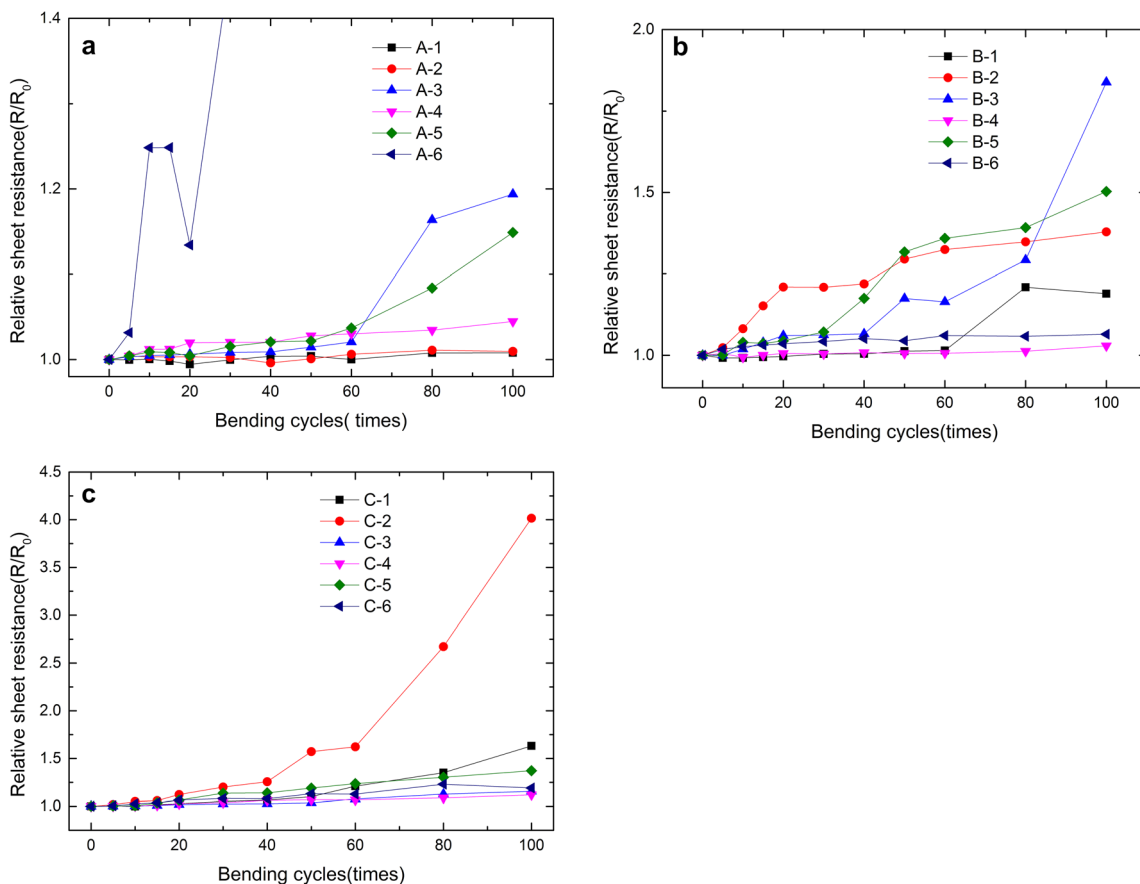


Fig. 9 Relationship of the relative sheet resistances with the bending cycles which the films experienced. The figures are respectively for samples deposited for **a** 10 min, **b** 20 min and **c** 30 min but at different temperatures

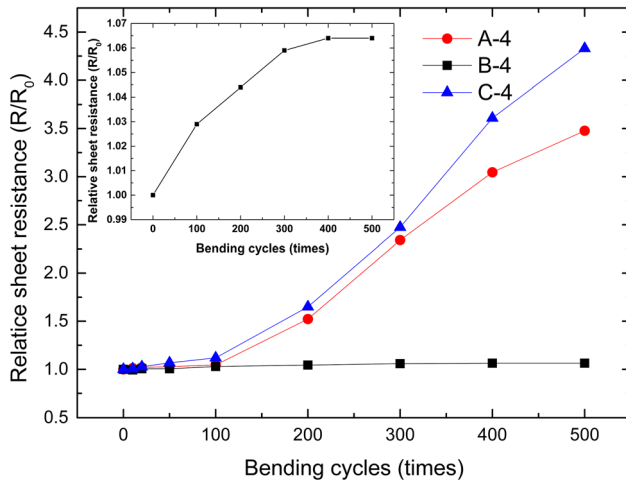


Fig. 10 Relative sheet resistance of samples with deposition temperature of 100 °C varies with bending 500 cycles. The inset shows an enlarge view of the B-4 curve

as-prepared sample (of sheet resistance $96.89 \text{ } \Omega/\text{cm}^2$), showing the film is of high mechanical stability, which meets the requirements in most applications to flexible devices.

It is noticed that the R/R_0 of B-4 increased rapidly during the initial bending process shown in the insert of Fig. 10, which may be caused by the following reason. Because of the expansion mismatch between doped CdO film and substrate, stress existed in the as-prepared film. During the initial bending cycles, the stress released by introducing defects and caused the rapid increasing of R/R_0 . After the stress released completely, the R/R_0 become steady.

3.5 Influence of substrates

To test the effect of different substrates on the electrical properties of the film, an In-doped CdO film was deposited on silicon substrate at 125 °C, for 20 min. Thus deposited sample had a sheet carrier concentration $1.24 \times 10^{16}/\text{cm}^2$, sheet resistance $35.86 \text{ } \Omega/\text{cm}^2$, and mobility $13.99 \text{ cm}^2/\text{V s}$. But the sample B-5 deposited under the same condition had a sheet carrier concentration of $6.69 \times 10^{15}/\text{cm}^2$, sheet resistance of $70.48 \text{ } \Omega/\text{cm}^2$ and mobility of $13.24 \text{ cm}^2/\text{V s}$. It is noticed that the sample deposited on silicon showed higher sheet carrier concentration. So the electrical properties of samples can be improved by selecting other substrates, which will be studied in further works.

4 Conclusion

In-doped CdO thin films were synthesized on PET substrate by RF magnetron sputtering. When the growth time was 20 min and the deposition temperature was 100 °C, the sample showed high transmittance of 75–98% in visible light region. The films also exhibited high mechanical stability. Without bending, its sheet resistance was $96.89 \text{ } \Omega/\text{cm}^2$, and after bending 500 times, the sheet resistance just increased by 6.4%. Under a bending curvature of 0.19 mm^{-1} , the sheet resistance of the film just increased by 11.3%. The transmittance of the films can be further increased by anti-reflection coating layers, such as ZnO film, TiO_2 film, Si_3N_4 film [35–40]. The effect of synthesis temperature and deposition time on the conductivity, transparency and mechanical stability of In-doped CdO films were studied in detail for the first time (Fig. 10).

Acknowledgements

This work was supported by the National Natural Science Foundation of China (Grant Nos. 11374280 and 50772110).

Author contributions

The experiment was designed under Prof. Guanzhong Wang's and Dr. Wei Zhu's help. Dr. Zishu Zhu finished the main part of the work and wrote this manuscript. Dr. Yanpu Chen cleaned PET substrates and finished the study about the variation of sheet resistance during 500 cycles of different samples, which was shown in Fig. 10. Dr. Pingping Ma and Dr. Haolei Zhou helped to put forward some valuable suggestions for experiment, such as how to test electrical properties of bending films. Dr. Liren Lou and Prof. Guanzhong Wang guided Dr. Zishu Zhu to complete the revision and the XPS analysis was designed under Dr. Liren Lou's advices.

Data availability

The data that support the finding of this study are available from the corresponding author upon reasonable request.

Declarations

Conflict of interest The authors declare that they have no conflict of interest.

Research involving human and animal rights This article does not contain any studies with human participants or animals performed by any of the authors.

Supplementary Information: The online version contains supplementary material available at <http://doi.org/10.1007/s10854-022-07745-5>.

References

1. T. Hanada, T. Negishi, I. Shiroishi et al., Plastic substrate with gas barrier layer and transparent conductive oxide thin film for flexible displays. *Thin Solid Films* **518**(11), 3089–3092 (2010)
2. D. Angmo, F.C. Krebs, Flexible ITO-free polymer solar cells. *J. Appl. Polym. Sci.* **129**(1), 1–14 (2013)
3. J.H. Kim, H.J. Seok, H.J. Seo et al., Flexible ITO films with atomically flat surfaces for high performance flexible perovskite solar cells. *Nanoscale* **10**(44), 20587–20598 (2018)
4. S.-I. Na, S.-S. Kim, J. Jo et al., Efficient and flexible ITO-free organic solar cells using highly conductive polymer anodes. *Adv. Mater.* **20**(21), 4061–4067 (2008)
5. C.P. Liu, C.Y. Ho, C.K. Kwok et al., High mobility transparent amorphous CdO-In₂O₃ alloy films synthesized at room temperature. *Appl. Phys. Lett.* **111**(7), 072108 (2017)
6. F. Li, Z. Lin, B. Zhang et al., Electrical and optical properties of flexible conductive carbon nanotube/Ag/Al-doped zinc oxide multilayer coatings. *Thin Solid Films* **525**, 93–96 (2012)
7. N. Sun, G. Fang, P. Qin et al., Efficient flexible organic solar cells with room temperature sputtered and highly conductive NiO as hole-transporting layer. *J. Phys. D Appl. Phys.* (2010). <https://doi.org/10.1088/0022-3727/43/44/445101>
8. Survey U S G. Mineral Commodity Summaries 2019:U.S. Geological Survey, 2019
9. W.-L. Jeong, J.-H. Min, H.-M. Kwak et al., A highly conductive and flexible metal mesh/ultrathin ITO hybrid transparent electrode fabricated using low-temperature crystallization. *J. Alloys Compd.* **794**, 114–119 (2019)
10. M.A. Shinde, K. Mallikarjuna, J. Noh et al., Highly stable silver nanowires based bilayered flexible transparent conductive electrode. *Thin Solid Films* **660**, 447–454 (2018)
11. C.-S. Chen, C.-K. Hsieh, An easy, low-cost method to transfer large-scale graphene onto polyethylene terephthalate as a transparent conductive flexible substrate. *Thin Solid Films* **570**, 595–598 (2014)
12. L.F. Lima, C.F. Matos, L.C. Gonçalves et al., Water based, solution-processable, transparent and flexible graphene oxide composite as electrodes in organic solar cell application. *J. Phys. D Appl. Phys.* **49**(10), 105106 (2016)
13. Y.-H. Chiang, C.-C. Peng, Y.-H. Chen et al., The utilization of IZO transparent conductive oxide for tandem and substrate type perovskite solar cells. *J. Phys. D Appl. Phys.* (2018). <https://doi.org/10.1088/1361-6463/aad71c>
14. M. Xie, W. Zhu, K.M. Yu et al., Effects of doping and rapid thermal processing in Y doped CdO thin films. *J. Alloys Compd.* **776**, 259–265 (2019)
15. A.A. Dakhel, Electrical and optical properties of iron-doped CdO. *Thin Solid Films* **518**(6), 1712–1715 (2010)
16. R.J. Stella, G.T. Rao, V.P. Manjari et al., Structural and optical properties of CdO/ZnS core/shell nanocomposites. *J. Alloys Compd.* **628**, 39–45 (2015)
17. R.K. Gupta, Z. Serbetci, F. Yakuphanoglu, Bandgap variation in size controlled nanostructured Li–Ni co-doped CdO thin films. *J. Alloys Compd.* **515**, 96–100 (2012)
18. L.J. Gao, S.F. Wang, R. Liu et al., The effect of Ni doping on the thermoelectric transport properties of CdO ceramics. *J. Alloys Compd.* **662**, 213–219 (2016)
19. R. Aydin, H. Cavusoglu, B. Sahin, Transition metal Mn/Cu co-doped CdO transparent conductive films: effect on structural, morphological and optical characteristics. *J. Alloys Compd.* **785**, 523–530 (2019)
20. N. Kati, Controlling of optical band gap of the CdO films by zinc oxide. *Mater. Sci. Pol.* **37**(1), 136–141 (2019)
21. A.A. Dakhel, Transparent conducting properties of samarium-doped CdO. *J. Alloys Compd.* **475**(1–2), 51–54 (2009)
22. K.M. Yu, D.M. Detert, G.B. Chen et al., Defects and properties of cadmium oxide based transparent conductors. *J. Appl. Phys.* **119**(18), 181501 (2016)
23. Z.G. Ji, M.M. Chen, P. Zhang et al., Deposition of low resistive transparent conducting Zn_xCd_{1-x}O films on flexible PET substrate at low temperature. *J. Inorg. Mater.* **23**(2), 361–363 (2008)
24. K. Nomura, H. Ohta, A. Takagi, T. Kamiya, M. Hirano, H. Hosono, Room-temperature fabrication of transparent flexible thin-film transistors using amorphous oxide semiconductors. *Nature* **432**, 488–492 (2004)
25. A.A. Dakhel, Structural, optical and electrical measurements on boron-doped CdO thin films. *J. Mater. Sci.* **46**(21), 6925–6931 (2011)
26. A.A. Dakhel, Impact of silicon doping on the properties of transparent conducting CdO thin films. *SILICON* **11**(1), 525–532 (2018)

27. A.A. Dakhel, Interfacial modification in Si/CdO heterojunction by Ge doping for optoelectronic applications. *Solid State Sci.* **25**, 33–38 (2013)
28. A.A. Dakhel, Electrical and Optical Investigations on Tungsten-Incorporated CdO Thin Films. *J. Electron. Mater.* **41**(9), 2405–2410 (2012)
29. Y.K. Zhu, R.J. Mendelsberg, J.Q. Zhu et al., Transparent and conductive indium doped cadmium oxide thin films prepared by pulsed filtered cathodic arc deposition. *Appl. Surf. Sci.* **265**, 738–744 (2013)
30. H. Kim, C.M. Gilmore, A. Piqué et al., Electrical, optical, and structural properties of indium–tin–oxide thin films for organic light-emitting devices. *J. Appl. Phys.* **86**(11), 6451–6461 (1999)
31. D.M. Smilgies, Scherrer grain-size analysis adapted to grazing-incidence scattering with area detectors. *J. Appl. Crystallogr.* **42**(Pt 6), 1030–1034 (2009)
32. S. Balamurugan, K. Usharani, D. Prabha et al., Ferromagnetism in CdO nanopowder—role of bioactive elements. *Mater. Lett.* **217**, 202–205 (2018)
33. J. Shruthi, N. Jayababu, P. Ghosal et al., Ultrasensitive sensor based on Y2O3-In2O3 nanocomposites for the detection of methanol at room temperature. *Ceram. Int.* **45**(17), 21497–21504 (2019)
34. P. Sakthivel, R. Murugan, S. Asaithambi et al., Influence of radiofrequency power on structural, morphological, optical and electrical properties of magnetron sputtered CdO:Sm thin films as alternative TCO for optoelectronic applications. *J. Alloys Compd.* **765**, 146–157 (2018)
35. S. Watanabe, T. Kodera, T. Ogihara, Influence of tellurite glass on reaction between Si₃N₄ anti-reflection coating film and Ag paste for electrodes in Si solar cells. *J. Ceram. Soc. Jpn.* **124**(3), 218–222 (2016)
36. A.S. Sarkin, N. Ekren, S. Saglam, A review of anti-reflection and self-cleaning coatings on photovoltaic panels. *Sol. Energy* **199**, 63–73 (2020)
37. S. Sali, S. Kermadi, L. Zougar et al., Nanocrystalline properties of TiO₂ thin film deposited by ultrasonic spray pulverization as an anti-reflection coating for solar cells applications. *J. Electr. Eng. Elektrotech. Casopis* **68**(7), 24–30 (2017)
38. J.Y. Chen, K.W. Sun, Growth of vertically aligned ZnO nanorod arrays as anti-reflection layer in silicon solar cells. *Sol. Energy Mater. Sol. Cells* **94**(5), 1078–1079 (2010)
39. E. Chanta, D. Wongratanaphisan, A. Gardchareon, et al., Effect of ZnO double layer as anti-reflection coating layer in ZnO dye-sensitized solar cells, in *International Conference on Alternative Energy in Developing Countries and Emerging Economies*, ed. by J. Waewsak, S. Othong, K. Sungkharak (Elsevier, 2015), pp. 879–884.
40. D.G. Chen, Anti-reflection (AR) coatings made by sol–gel processes: a review. *Sol. Energy Mater. Sol. Cells* **68**(3–4), 313–336 (2001)

Publisher's Note Springer Nature remains neutral with regard to jurisdictional claims in published maps and institutional affiliations.